

# The Role of Mitochondrial VDAC2 in the Survival and Proliferation of T-Cell Acute Lymphoblastic Leukemia Cells

Filippus lipinge Tshavuka<sup>1,2\*</sup>, Lin Zou<sup>1,3</sup>

<sup>1</sup>Center of Clinical Molecular Medicine, Children Hospital of Chongqing Medical University, Chongqing, China

<sup>2</sup>School of Medicine, University of Namibia, Windhoek, Namibia

<sup>3</sup>Clinical Research Unit, Children's Hospital of Shanghai Jiao Tong Medical School, Shanghai, China

Email: \*feitshavuka@gmail.com

**How to cite this paper:** Tshavuka, F.I. and Zou, L. (2023) The Role of Mitochondrial VDAC2 in the Survival and Proliferation of T-Cell Acute Lymphoblastic Leukemia Cells. *Journal of Biosciences and Medicines*, 11, 265-283.

<https://doi.org/10.4236/jbm.2023.1110024>

**Received:** August 28, 2023

**Accepted:** October 28, 2023

**Published:** October 31, 2023

Copyright © 2023 by author(s) and Scientific Research Publishing Inc.

This work is licensed under the Creative Commons Attribution International License (CC BY 4.0).

<http://creativecommons.org/licenses/by/4.0/>



Open Access

## Abstract

**Background:** T-cell acute lymphoblastic leukemia (T-ALL) is an aggressive hematological malignancy with aberrant T-cell developmental arrest. Individuals with relapsed T-ALL have limited therapeutic alternatives and poor prognosis. The mitochondrial function is critical for the T-cell viability. The voltage-dependent anion channel 2 (VDAC2) in the mitochondrial outer membrane, interacts with pro-apoptotic BCL-2 proteins and mediates the apoptosis of several cancer cell lines. **Objective:** The aim of the current study is to explore the role of VDAC2 in T-ALL cell survival and proliferation. **Methods:** Publicly available datasets of RNA-seq results were analyzed for expression of VDAC isoforms and T-ALL cell lines were treated with a VDAC2 small molecular inhibitor erastin. A VDAC2 RNA interference (siRNA) was delivered to T-ALL cell lines using a retroviral vector. Functional assays were performed to investigate the VDAC2 siRNA impacts on cell proliferation, apoptosis and survival of T-ALL cells. **Results:** Our analysis found a high expression of VDAC2 mRNA in various T-ALL cell lines. Public datasets of T-ALL RNA-seq also showed that VDAC2 is highly expressed in T-ALL (116.2 ± 36.7), compared to control groups. Only two T-ALL cell lines showed sensitivity to erastin (20 µM) after 48 hours of incubation, including Jurkat (IC<sub>50</sub> = 3.943 µM) and Molt4 (IC<sub>50</sub> = 3.286 µM), while another two T-ALL cells (CUTLL1 and RPMI 8402) had unstable IC<sub>50</sub>. However, five T-ALL cell lines (LOUCY, CCRF-CEM, P12-ICHI, HPB-ALL, and PEER cells) showed resistance to erastin. On the contrary, all T-ALL cell lines genetically inhibited with VDAC2 siRNA led to more than 80% decrease in VDAC2 mRNA levels, and a < 80% decrease in viability of cells transfected. The siRNA specific to VDAC2, also led to suppressed proliferation and induced a sub-G1 cell cycle

arrest of T-ALL cells. **Conclusion:** VDAC2 is highly expressed in T-ALL cells. The inhibition of VDAC2 significantly decreased cell viability, increased apoptosis, reduced cell proliferation and caused cell cycle sub-G1 arrest of T-ALL cells.

## Keywords

VDAC2, Mitochondrial-Mediated Apoptosis, T-Cell Acute Lymphoblastic Leukemia

---

## 1. Introduction

T-cell acute lymphoblastic leukemia (T-ALL) is a complex heterogeneous malignancy, with an aberrant T-cell developmental arrest. Acute lymphoblastic leukemia (ALL) is divided according to two lymphocyte lineages: B-ALL (B cell-derived ALL) and T-ALL (T cell-derived ALL) [1]. ALL is generally predominant in children than adults as 80% of ALL cases are found in children [2] [3].

T-ALL only represents about 12% - 15% of cases of all newly diagnosed ALL pediatric patients [4]. However, it represents a problematic, high-risk type of leukemia. Firstly, a significant number of cases suffer from primary resistance [5], following an intensified multi-agent chemotherapy regimen. Secondly, patients who respond to initial treatment eventually suffer from a relapse accompanied by a poor prognosis [2] [4]. Therefore, the key to improving the prognosis of T-ALL is to reveal possible new therapeutic targets.

The function of mitochondria is critical in T-cell development [6]. In cancer cells, the mitochondrion, is the “powerhouse” of cancer cells, as it generates energy for cells through its flexible bioenergetic profile of being able to switch malignant cells between aerobic glycolysis and oxidative phosphorylation (OXPHOS), thereby ensuring a rapid anabolism [3] [7]. The mitochondria also participate in cellular fate decisions. In this way, the mitochondria maintain the viability of malignant cells, and promote the oncogenic transformation of malignant cells [3]. Cancerous cells employ mechanisms to protect malignant cells from activation of apoptosis signals [8] [9]. Mitochondrial outer membrane permeabilization (MOMP) is involved in the influx of calcium ( $Ca^{2+}$ ) and consequent cell death during normal T-cell development [6]. MOMP causes the release of cytochrome C and SMAC/DIABLO, which then activates the caspase cascade and cell death. A lot of genes affect the normal function of mitochondria.

The mitochondrial VDAC2-BAK axis has been shown to influence the negative selection of thymocytes and thymocyte survival in the thymus during T-cell thymopoiesis [6]. This axis eventually evokes mitochondrial-mediated apoptosis by triggering a calcium flux upon TCR engagement. This in turn initiates the deletion of self-directed thymocytes [6]. Most tumor cells capitalize on their ability to protect themselves against cell death [8] [10]. However, the role of VDAC2-BAK axis in propagating of malignant transformation and protecting of

tumors from cell death in T-cell acute lymphoblastic leukemia remains elusive [6].

All three VDAC isoforms have redundant and substitutable roles in the metabolic and ion flux [11]. However, VDAC1 and VDAC2 have isoform-specific roles, and diametrically opposed functions in mitochondrial-mediated apoptosis. VDAC1 isoform has pro-apoptotic roles while VDAC2 has anti-apoptotic/pro-survival roles [6] [7] [10] [12] [13]. The non-redundant roles of VDAC2 in either mediating or preventing apoptosis are not yet fully understood and still remain controversial [7] [10]. Mice embryos with homozygous VDAC2 allele deletion died during development, whereas embryos with deletion of the other two isoforms, VDAC1 and VDAC3, survived [11]. The VDAC2 binds BAK/BAX complex, and keeps it in an inactive form. When released, it leads to homodimerization of BAK and interactions that culminate in MOMP and cell death [6] [10] [12] [14] [15] [16]. Therefore, it is very important to analyze the expression patterns of VDAC isoforms in T-ALL as well as the T-cell developmental stages. And still, no published study is available that has looked at the pro-survival VDAC2 role [16] [17] in T-cell acute lymphoblastic leukemia.

The main goal of the study was to analyze the expression patterns of VDAC isoforms in T-ALL when compared to control cells, explore whether inhibition of VDAC2 in T-ALL is pro-apoptotic or pro-survival (anti-apoptotic), and explore the inhibition of VDAC2 using RNA interference (RNAi) as a therapeutic strategy in the treatment of T-cell acute lymphoblastic leukemia (T-ALL).

Using RNA-seq data and VDAC2 inhibitors, it was found that VDAC2 is highly expressed in T-ALL cells. Inhibiting VDAC2 led to a significant reduction in cell viability, increased apoptosis, decreased cell proliferation, and induced cell cycle sub-G1 arrest in T-ALL cells.

## 2. Materials and Methods

### 2.1. RNA-Seq Datasets

To compare the global expression of different VDAC isoforms in different physiological T lymphoid tissues to the malignant T-ALL, we used publicly available GEO datasets (GSE141140, GSE33470) extracted from the website <https://www.ncbi.nlm.nih.gov/gds> and analyzed in GraphPad prism 9.0. The dataset GSE141140 was modified in our lab, in a different study, to add more control groups, namely the thymocytes and hematopoietic pluripotent stem cells (HPSCs) respectively. For differential gene analysis and protein-to-protein interaction, we used Cytoscape and R software respectively.

### 2.2. Cell Culture

T-ALL cell lines: Jurkat, Molt4, Loucy, CUTLL1, RPMI 8402, CCRF-CEM, P12-Ichikawa (P12 or P12-Ich), HPB-ALL, Peer and Molt3 cells, kindly provided by the Center of Molecular Medicine, Children's Hospital of Chongqing Medical University, were cultured in RPMI 1640 (Gibco, USA) supplemented with 10%

FBS, 1% penicillin/streptomycin combo (Gibco, USA), and 2 mmol/l L-glutamine. T-ALL cell lines were treated with inhibitors of VDAC2.

HEK-293PA (Human embryonic kidney) cells kindly provided by the Center of Molecular Medicine, Children's Hospital of Chongqing Medical University, were grown in Dulbecco's modified Eagle's medium (DMEM) (Gibco, USA), which included 10% FBS, 1% penicillin/streptomycin combination, and 2 mmol/l L-glutamine, were used to produce the retrovirus expression vector. All cells were cultured in a humidified atmosphere at 37°C in 5% CO<sub>2</sub>. This cell line was used to assemble retroviral vector particles, containing siRNA.

### 2.3. Total RNA Extraction

About  $2 \times 10^6$  cells were centrifuged at 800 G/min, 4°C; supernatant was completely removed, and 1 ml of Trizol RNAiso (Takara, Japan) was added, mixed well then 200 µl Trichloromethane was added, mixed well again and centrifuged at 4°C for 13,000 G for 15 minutes. The tRNA will be found in the supernatant. After centrifugation, 400 µl of supernatant is carefully aspirated into a new vial after which same volume of isopropanol is added and mixed homogeneously; centrifuged at 4°C for 13,000 G for 10 minutes. The supernatant is discarded and do the wash step twice with freshly prepared 70% ethanol, by centrifuging at 4°C, 12,000 rpm for 5 minutes; completely discard supernatant by spinning down on the mini-centrifuge for 5 seconds and aspirate with pipet and dry at room temperature for 5 minutes. 10 µL of ddH<sub>2</sub>O is added to dissolve tRNA; then detect extracted RNA by agarose gel electrophoresis.

### 2.4. Detection of VDAC2 mRNA by Real-Time Quantitative PCR (RT qPCR)

The cDNAs were treated to SYBR Green-based real-time PCR method, and GAPDH was used as reference gene. The following primer sequences for gene expression RT qPCR assays were used: Human *VDAC2*, forward: CTTTGCAGT GGGCTACAGGA, reverse: ACGAGTGCAGTTGGTACCTG; GAPDH forward: CAGCGACACCCACTCCTCCACCTT, reverse: ATGAGGTCCACCACCCTGTTGCT.

### 2.5. Inhibition of VDAC2 by Erastin and Cell Viability Testing

The T-ALL cell lines were cultured in presence of erastin at increasing concentration (from 0 µM to 20 µM), at 37 °C in 5% CO<sub>2</sub> for 48 hours, then tested using PE Annexin V method, as described by manufacturer provided protocol.

### 2.6. Small Interfering RNA (siRNA) and Molecular Cloning

The siRNA construct of human VDAC2 was designed and procedure was performed as reported elsewhere [18]. The hVDAC2-siRNAs were synthesized by Huada Biology (Beijing, China) and then used in molecular cloning step. The following sequences were used:

Sense: **GGCAAAAAA** GCTTGGACATCAGGTACCAACTGCA **TTTTT**,

Antisense: **GCCA AAAAAAT**GCAGTTGGTACCTGATGTCCAAGC **TTTTT**.

An in-house plasmid, pSEIB-361-GFP, was cut using a single point restriction endonuclease enzyme (NEB, USA), linked to siRNA construct with T4 DNA ligase (NEB, USA) to form a recombinant DNA sequence. 50  $\mu$ l *E. coli* DH5 $\alpha$  (Tiangen, CAT: CB101) competent cells were transformed with recombinant DNA sequence, by heat shock at 42°C for 90 seconds, to allow penetration of expression vector containing target sequence, placed on ice for 3 - 5 minutes; then mixed with 800  $\mu$ l liquid broth and shaken in a water bath at 37°C for 30 - 60 minutes. Transformed cells are then centrifuge at 2000 rpm for 3min, and sediment of competent cells is evenly spread on Muller-Hinton plate coated with Ampicillin (concentration of 100 mg/ml) and incubates it at 37°C for 12 - 14 hours. Plasmid is extracted from single colonies bacteria by alkaline lysis method, followed by agarose gel electrophoresis, plasmid PCR, and RNA depletion by magnetic beads, using manufacturer provided protocol.

## 2.7. Production of Retrovirus

The HEK-293PA cell was cultured in T7 flasks until it reaches 60% - 80% confluence. Transfection was done for each of the three plasmids: 8  $\mu$ g of recombinant p-SEIB-361-GFP-hVDAC2-siRNA; packaging plasmids: 8  $\mu$ g of p-Ampho and 2  $\mu$ g of p-VSV-g. 144  $\mu$ g of polyethylenimine (PEI) reagent (Polysciences, Warrington, USA), was used to enhance transfection efficiency. The first four hours, FBS-free DMEM was used, followed by DMEM supplemented by 10% FBS for 24 h, then replaced with fresh media. Supernatants with retrovirus were collected at 48 h, 72 h and 96 h from HEK-293PA cells, post-transfection for harvesting of retrovirus vectors.

### Retroviral infection of T-ALL cells for siRNA gene delivery

Healthy T-ALL cell lines with at least 70% confluence were centrifuged and resuspended in fresh, serum-free RPMI 1640 medium. The supernatant containing retrovirus was infected together with 4  $\mu$ g/ml Polybrene (Polysciences, Warrington, USA) to cells in 3 cycles at 4 h intervals, virus was reinfected into cells three times, and replacing the media with each round. The infected cells were screened at 48 h post-infection according to the different tolerance concentration of blasticidin (Polysciences, Warrington, USA).

## 2.8. Cell Viability and Apoptosis Measurement by PE Annexin V

About  $5 \times 10^5$  cells were centrifuged at 2000 rpm for 5 minutes, and the supernatant was removed. Pre-cooled PBS was added to the cells, and they were spun at 2000 rpm for 5 minutes to wash them. PE Annexin V method was performed according to manufacturer provided protocol.

## 2.9. Cell Proliferation Measurement by CCK-8

To test cell viability and deduce cell proliferation rate, T-ALL cells in logarithmic

growth phase after exposure to various treatment factors were inoculated on 96 well plates at rate of 5000 cells per well, with 3 wells per group. After 12 h, 24 h, 48 h, 72 h respectively, 10  $\mu$ l CCK-8 solution is added to each well, mix before continuing to culture. After 4 h, absorbance at wavelength of 450 nm was detected by an enzyme marker. A cell proliferation curve based on absorbance values was drawn.

### 2.10. Cell Cycle Detection by Propidium Iodide (PI) Staining

Cell cycle was tested 48 h and 72 h after exposure to treatment factors. T-ALL cells were isolated and rinsed in PBS; fixed with 70% ethanol and PI staining was performed according to manufacturer protocol.

### 2.11. Statistical Analysis

To unless otherwise stated, all experiments performed in triplicates. Statistical details of the experiments including statistical tests used can be found in the figure legends. Statistical significance was defined as  $p < 0.05$ . We used GraphPad 9.0 software to analyse our experimental and public dataset data. All experiments, when  $n$  not indicated, were carried out in triplicates and a mean value was taken as a final value. Experimental data were analyzed using the statistical methods: Student's t-test or repeated-measures one-way or two-way analysis of variance (ANOVA) as indicated in the figure legends.

## 3. Results

### 3.1. Expression of VDAC Isoforms in Normal Lymphoid Tissues vs. in T-ALL

Our observations were that the global expression levels (mean  $\pm$  SD) of VDAC2 were highest expressed isoform in T-ALL cells ( $116.2 \pm 36.7$ ) when compared to the control group cells, which are: the thymocytes, HPSC and normal T lymphocytes (peripheral T lymphocytes). VDAC1 was the highest expressed isoform in the control group, HPSC ( $90.7 \pm 42.9$ ) and thymocytes ( $150.1 \pm 33.9$ ). On the other hand, VDAC3 showed no statistically-significant difference in the mean value across all cell types (**Figure 1(A)** & **Figure 1(B)**).

VDAC2 expression in T-ALL patients' cells was significantly high, compared to VDAC2 expression in normal peripheral T cells ( $p < 0.0027$ ). There was no significant difference in levels of VDAC2 between T-ALL cells when compared to HPSC ( $p < 0.2159$ ), and thymocytes ( $p < 0.3713$ ). Interestingly, VDAC1 isoform expressed the same pattern, with comparable means between T-ALL cells against HPSCs ( $p < 0.4067$ ) and thymocytes ( $p < 0.0879$ ) and a significantly lower VDAC1 expression in peripheral T lymphocytes ( $p < 0.0008$ ) (**Figure 1(A)** & **Figure 1(B)**).

We then tested mRNA expression of VDAC2 by quantitative RT-PCR, amongst seven T-ALL cell lines, namely Jurkat, Molt4, CUTLL1, RPMI 8402, CCRF-CEM, HPB-ALL, and P12-ICH cells, and found that VDAC2 was heterogeneously

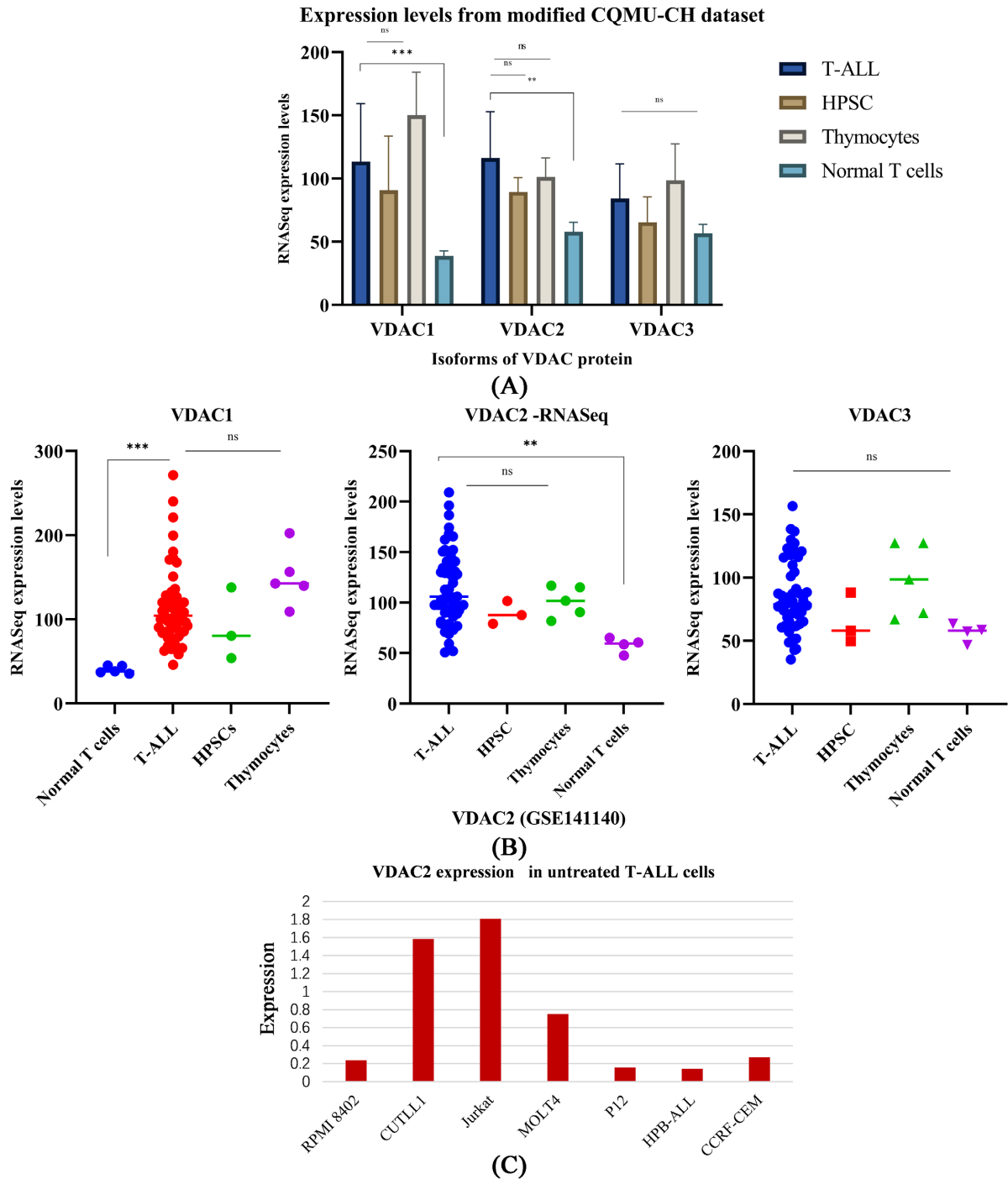


**Figure 1.** Global expression of VDAC isoforms in lymphoid cells compared to T-ALL cells. ((A), (B)) RNA-seq expression levels of VDAC isoforms in T-ALL cells compared to control groups. (C) An RT qPCR expression of VDAC2 in different T-ALL cell lines. CQMU-CH: Chongqing Medical University-Children’s Hospital; T-ALL: T-cell acute lymphoblastic leukemia; HPSCs: hematopoietic progenitor stem cells; P12: P12-Ichikawa. \* $p < 0.05$ ; \*\* $p < 0.001$ ; \*\*\* $p < 0.0001$ ; ns: p-value non-significant.

expressed in T-ALL cell lines.

### 3.2. VDAC2 Expression at Different Stages of T-Cell Development

In **Figure 2**, we investigated how VDAC2 is expressed in developing T cells,

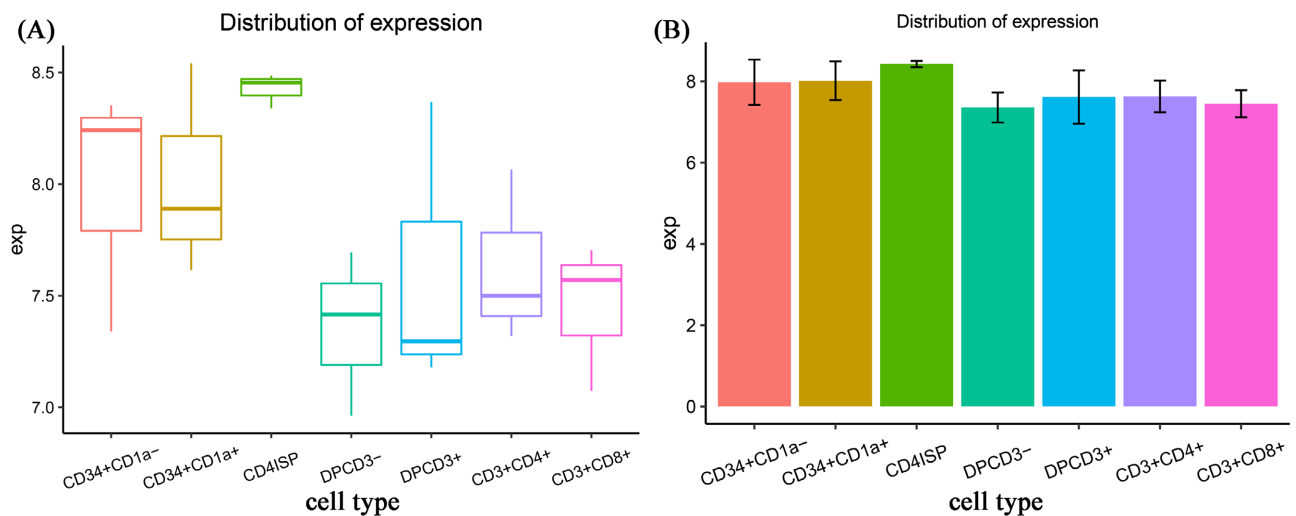


**Figure 2.** Expression of VDAC2 at different T-cell development stages (dataset GSE33470). ((A), (B)) Graphical expression of VDAC2 in normal thymocytes, at different stages of thymopoiesis, shows higher expression of VDAC2 in undifferentiated or poorly differentiated double negative thymocytes (CD34<sup>+</sup>CD1a<sup>-</sup> to CD4ISP) than when compared to more differentiated thymocytes. T-ALL: T-cell acute lymphoblastic leukemia; HPSCs: hematopoietic progenitor stem cells.

from the bone marrow, through thymus into the peripheral blood. Using publicly available dataset (GSE33470) RNA-seq results, we found that VDAC2 expression levels were the highest at the intermediate single positive stage (ISP), which is a transitioning stage between double negative (DN) and double positive (DP) stages. Comparing the expression of VDAC2 in a poorly differentiated and immature double negative thymocytes stage (CD34<sup>+</sup>CD1a<sup>-</sup> to CD4ISP) to the more differentiated, DP and single positive cells (DP3CD3<sup>-</sup> to CD3<sup>+</sup>CD8<sup>+</sup>), we found a significant difference in expression ( $p < 0.0040$ ).

### 3.3. VDAC2 Interacts with Genes Associated with Mitochondria Mediated Apoptosis

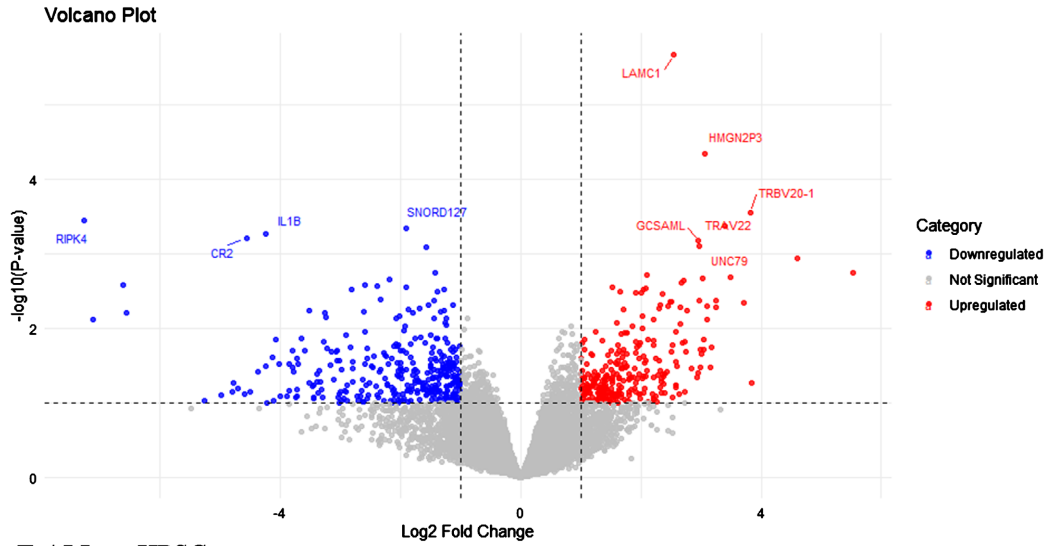
Using the RNA-seq dataset results (GSE141140), we found that protein to protein interactions of VDAC2 existed with other genes associated with mitochondria-mediated apoptosis pathway. **Figure 3** shows that VDAC2 is associated to 5 genes, namely BAK, BAX, BCL2-L1, CASP3 and DIABLO. Further differential genomic analysis of the dataset revealed that different gene expression existed in the three different controls when compared to T-ALL, indicating that the type of control is very important when comparing the gene expression of different cohorts.

### 3.4. Inhibition of VDAC2 by a Small Molecular Inhibitor Erastin

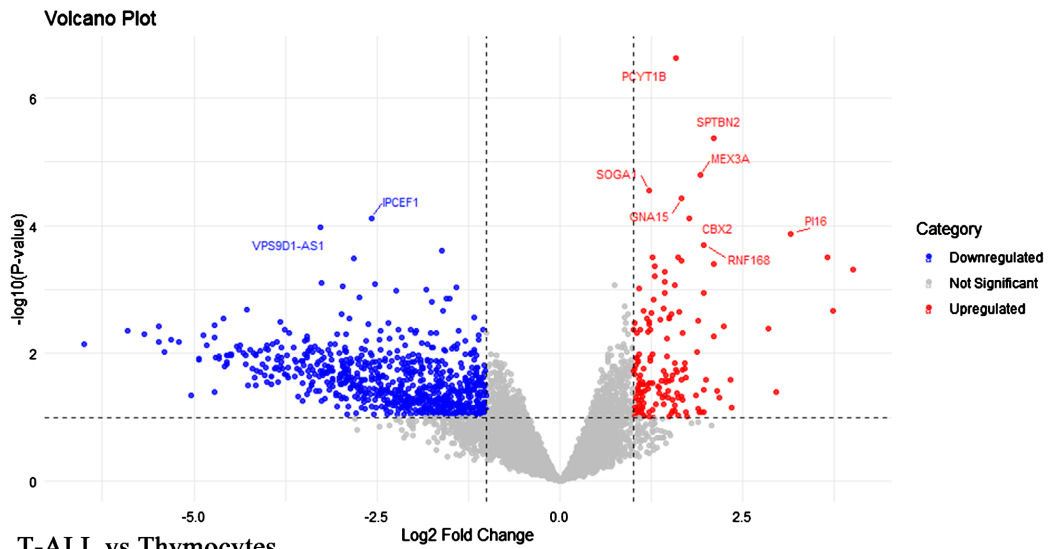
We tested the effects of inhibiting *VDAC2* in T-ALL cell lines, using a small molecular inhibitor erastin, at increasing concentration (0, 0.1, 1.0, 5.0, 10, 20  $\mu$ M), after incubation for 48 hours at 37°C in CO<sub>2</sub>. The cell survival rates as measured by PE Annexin V flow cytometry method, as demonstrated in **Figure 4**, shows that two cell lines (Jurkat with IC<sub>50</sub> = 3.943  $\mu$ M, Molt4 with IC<sub>50</sub> =



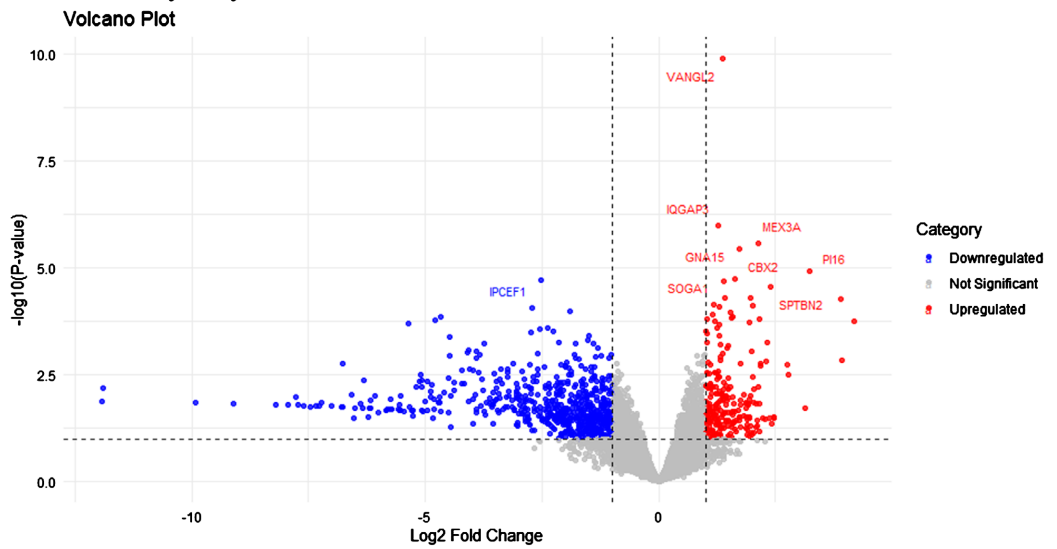
### T-ALL vs Normal T cells



### T-ALL vs HPSC



### T-ALL vs Thymocytes



(A)

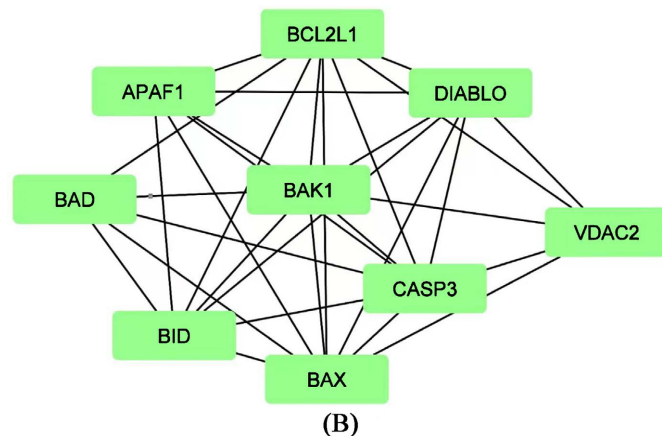


**Figure 3.** Differential genomic analysis of modified dataset GSE141140. (A) Volcano plots comparing T-ALL cells to control groups: thymocytes, HPSC and peripheral T lymphocytes. Different genes different gene expression existed in the three different controls. (B) Protein-to-protein interaction analysis found 5 genes involved in mitochondrial-mediated apoptosis directly interact with VDAC2.

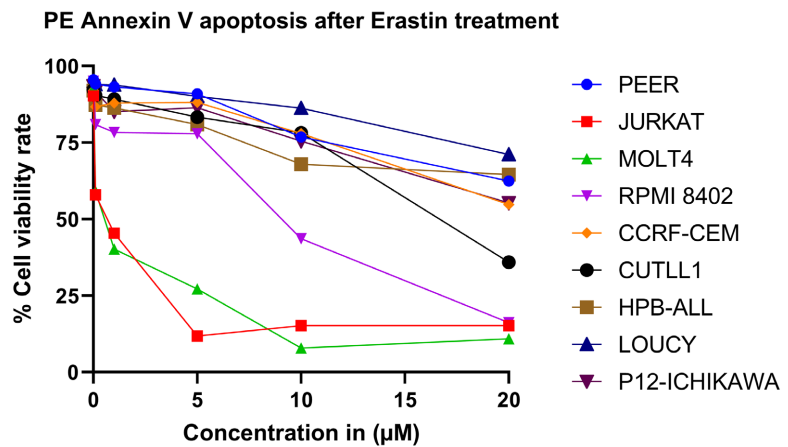


**Figure 4.** Cell survival rates 48 h after treatment with erastin. Only two cell lines (Jurkat with  $IC_{50} = 3.943 \mu M$ , Molt4 with  $IC_{50} = 3.286 \mu M$ ) showed sensitivity to erastin. Two more cell lines showed unstable  $IC_{50}$  (CUTLL1 and RPMI 8402) and five showed resistances to erastin (Loucy, CCRF-CEM, P12-ICHIKAWA, HPB-ALL, and PEER cells).

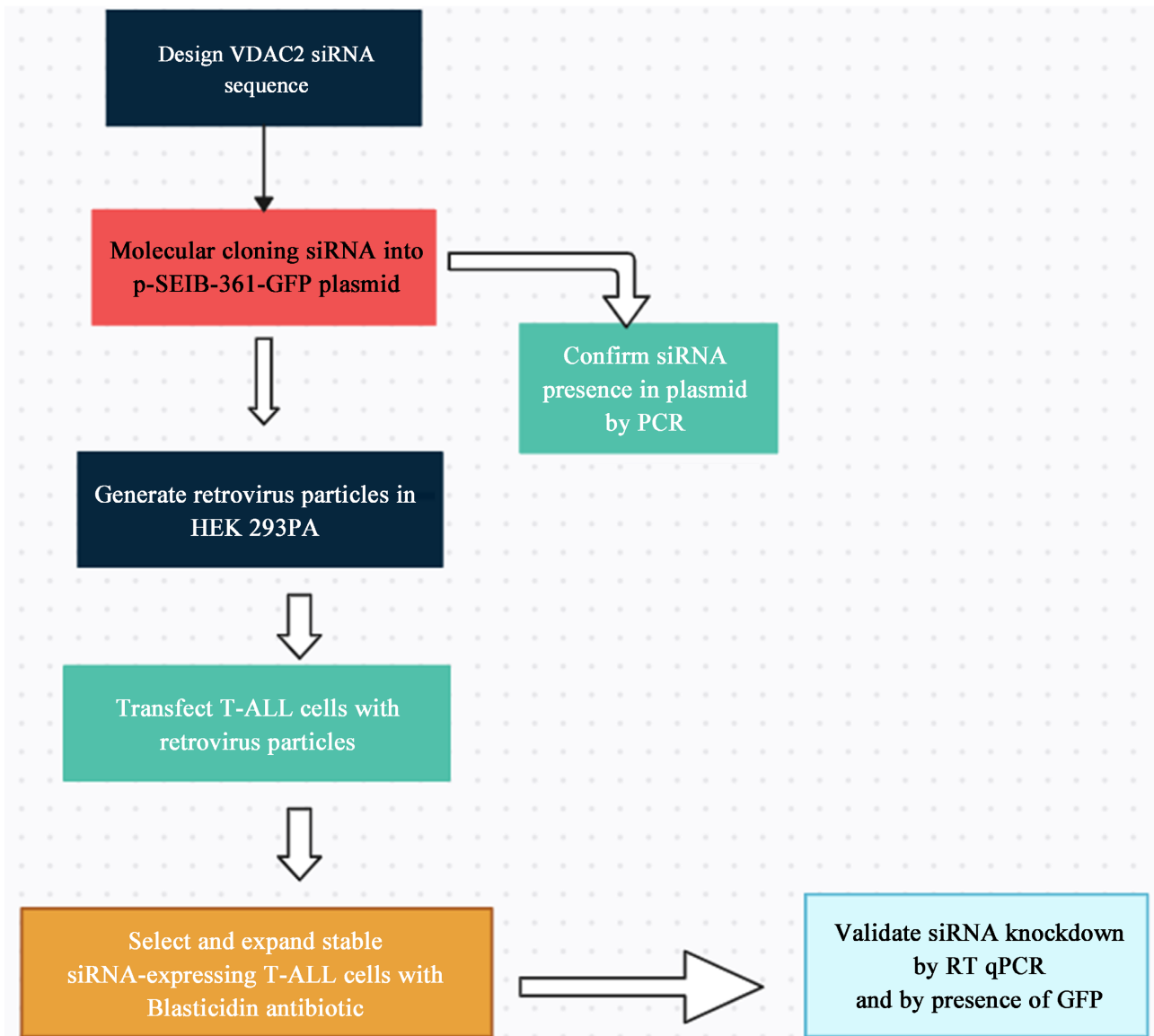
3.286  $\mu M$ ) were sensitive to erastin and the rest cell lines either had unstable  $IC_{50}$  (CUTLL1 and RPMI 8402) or showed resistance to erastin (Loucy, CCRF-CEM, P12-ICHI, HPB-ALL, and PEER cells).

### 3.5. Genetic Silencing of VDAC2 with siRNA Reduced Cell Survival Rate and Proliferation

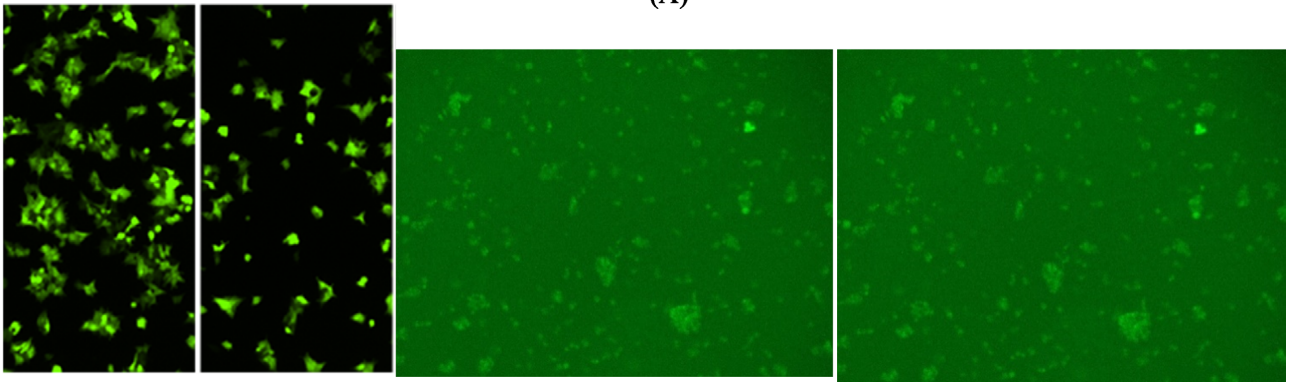
To investigate the cell viability and proliferation of T-ALL cells when cells are exposed to transient silencing of the VDAC2 gene, thereby creating stably expressing VDAC2-siRNA cells (see **Figure 5**). We measured the functional effects such as survival, apoptosis and proliferation rate of T-ALL cells transfected with siRNA over a period of 96 hours.

Using the CCK-8 assay, we found that T-ALL cells showed a gradual increase

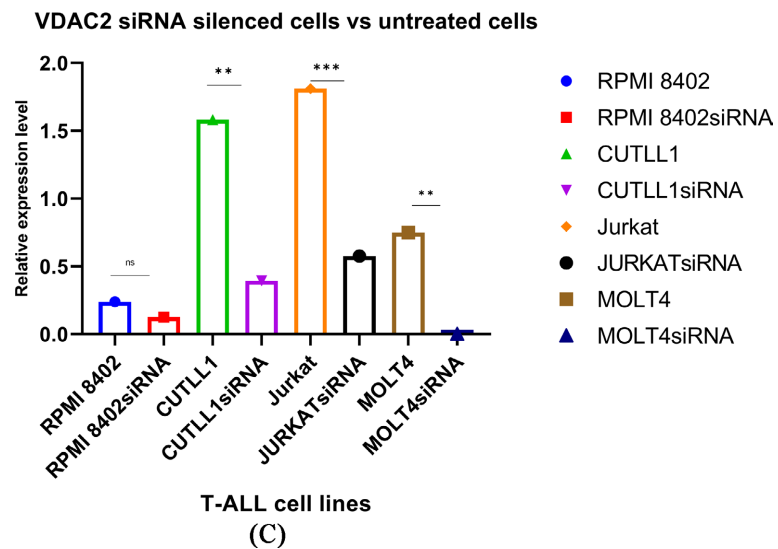
## Workflow chart for creating stable VDAC2-siRNA cells



(A)



(B)



Note: ns: not significant p-value; \*\* $p < 0.001$ ; \*\*\* $p < 0.0001$ .

**Figure 5.** Creating a stable VDAC2 siRNA-expressing retrovirus T-ALL cells. (A) Experimental workflow for creating a stable VDAC2 siRNA-expressing retrovirus T-ALL cells. (B) HEK-293PA cells for producing retrovirus vector, 48 hours post-transfection with plasmids; and Jurkat, Molt4 cells 48 hours post-VDAC2-siRNA delivery. (C) RT qPCR quantification of VDAC2 mRNA before and 72 hours after VDAC2-siRNA transfection showing successful knockdown of VDAC2.

in proliferation for the first 48 hours post-transfection, followed by an abrupt abrogated proliferation which was pronounced at 96 hours post-siRNA transfection (see **Figure 6(A)**). A decreased cell survival rate and increased apoptosis was also confirmed by PE Annexin V method, 96 h post-transfection (**Figure 6(B)** & **Figure 6(D)**). The results indicated that VDAC2 siRNA took effect at 48 hours after transfection. When comparing the proliferation rates as measured in absorbance of cells at 72 hours and 96 hours post-transfection, there is an inhibited proliferation ( $p < 0.0016$ ).

We further went to confirm the survival and apoptosis rate of T-ALL cells post-transient silencing of VDAC2 with siRNA by means of PE Annexin V assays. Six VDAC2 siRNA transfected cells showed a decreased cell viability to an average of <20%, 72 hours after retrovirus was introduced. When we compared the mean survival rate of all cell lines at zero hours before transfection (mean 94.4%,  $\pm 1.90$ ) and 72 hours after transfection (mean 12.0%,  $\pm 4.67$ ) by ANOVA, the difference was very statistically significant ( $p < 0.0001$ ).

### 3.6. VDAC2 siRNA Treated Cells Show a Sub-G Cell Cycle Arrest

We stained T-ALL cells with Propidium Iodide, to determine the cell cycle status of cells with genetic downregulated of VDAC2. Surprisingly, treatment of T-ALL cells with VDAC2 siRNA arrested cell cycle in Sub-G<sub>1</sub> phase, for all the six cell lines tested. When comparing cell cycle of untreated to VDAC2-siRNA treated T-ALL cells, there is a decrease in the proportion of cell cycle division, namely the G<sub>1</sub>-phase, S-phase and G<sub>2</sub>-phase (**Table 1(A)** & **Table 1(B)**; **Figure 7**). Most

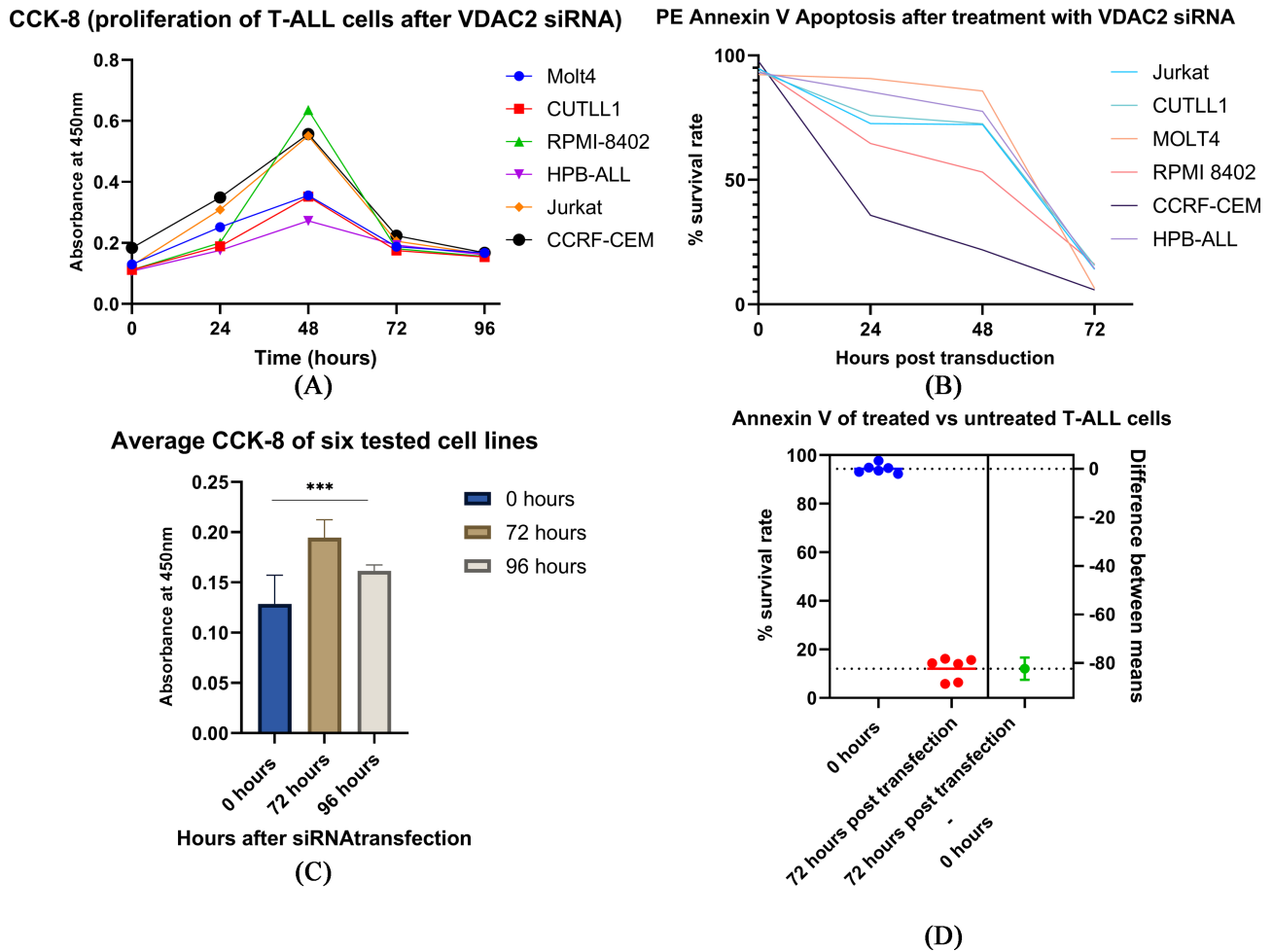


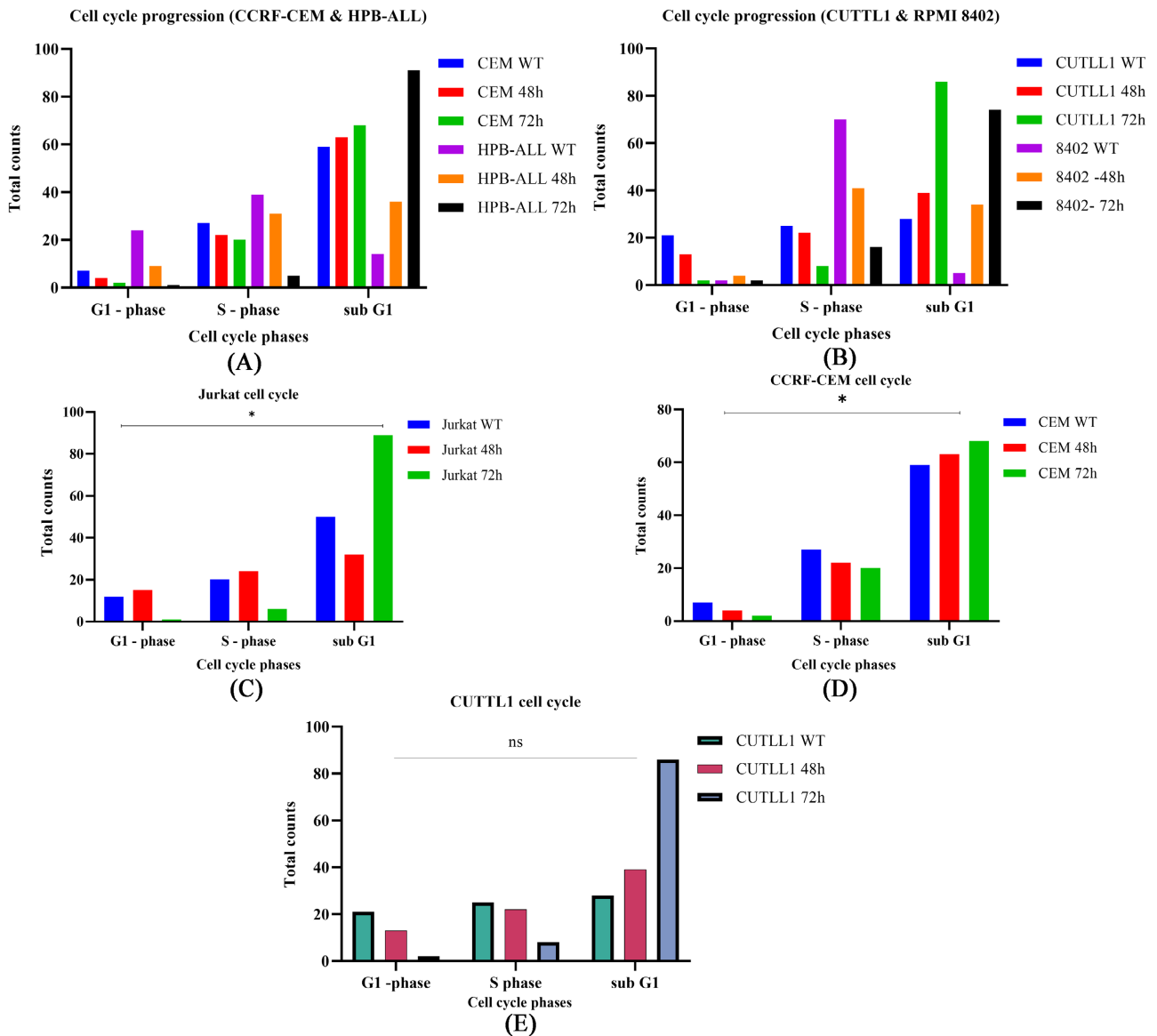
**Figure 6.** VDAC2 siRNA-expressing T-ALL cells show dramatic decreased in survival and proliferation rate and increased apoptosis rate. (A) CCK-8 assays, and (B) Annexin V assay showing the dramatic decrease in proliferation from 42 hours post-knockdown. (C) Comparison of cell viability by ANOVA at 0, 72 and 96 hours post-knockdown was statistically significant ( $p < 0.0001$ ). (D) Estimation plot comparing cell viability at 0 and 72 hours post-VDAC2 knockdown (student's t-test  $p < 0.0001$ ). \* =  $p < 0.05$ ; \*\* =  $p < 0.001$ ; \*\*\*  $p < 0.0001$ ; ns: p-value non-significant.

**Table 1.** (A) Cell cycle progression in T-ALL cell lines (CUTLL1, RPMI 8402, HPB-ALL) with VDAC2 knockdown; (B) Cell cycle progression in T-ALL cell lines (Jurkat, Molt4, CCRF-CEM) with VDAC2 knockdown.

(A)									
	CUTLL1 WT	CUTLL1 48 h	CUTLL1 72 h	8402 WT	8402-48 h	8402-72 h	HPB-ALL WT	HPB-ALL 48 h	HPB-ALL 72 h
G1-phase	21.2	13.9	2.34	2.49	4.35	2.44	24.7	9.07	1.03
S-phase	25.1	22.9	8.24	70.1	41.9	16.7	39.2	31.9	5.45
Sub-G1	28	39.1	86.6	5.27	34	74.6	14.4	36.1	91.7

(B)									
	Jurkat WT	Jurkat 48 h	Jurkat 72 h	Molt4 WT	Molt4 48 h	Molt4 72 h	CEM WT	CEM 48 h	CEM 72 h
G1-phase	12.6	15	1.54	13.2	1.22	2.73	7.46	4.75	2.38
S-phase	20.3	24.5	6.31	58.4	68.3	39.3	27	22.5	20.9
Sub-G1	50.8	32.2	89.3	-0.87	12.1	43.3	59.5	63.4	68.4



**Figure 7.** Cell cycle progression after genetic knockdown of VDAC2. ((A), (B)) A summary of cell cycle status in four different cell lines measured when untreated, at 48 hours and 72 hours after transfection with VDAC2-siRNA. All cells show accumulation of cells in sub-G1 phase and dramatic decrease in the S-phase 72 hours post-transfection, indicating a cell cycle arrest in sub-G1 phase. (C)-(E) Paired student’s t-test comparison in cell cycle progression in Jurkat (C), CCRF-CEM (D) and CUTLL1 (E) cells, respectively. \* $p < 0.05$ ; ns: not significant p-value.

of the cells were confined to the sub-G1 phase of cell cycle and facing an imminent cell death. Transfection of T-ALL cells with VDAC2-siRNA induced a G0/G1 cell cycle arrest (Figure 7; Table 1(A) & Table 1(B)). We then used student’s t-test to compare of flow cytometry counts (G1 phase compared to sub-G1 phase) of all six tested cell lines when untreated with VDAC2-siRNA to 72 hours post-treatment we found that statistically significant values in Jurkat ( $p < 0.05$ ) and CCRF-CEM cells ( $p < 0.05$ ), and a non-significant p-value but elevated sub-G1 cell population in Molt4, HPB-ALL, RPMI 8402 and CUTLL1 cells.

## 4. Discussion and Conclusions

The function of mitochondrial porin VDAC as a passage for metabolites and ions has been extensively studied; however, just how VDAC2 interacts with BCL-2 proteins to mediate apoptosis is poorly understood in leukemia. Here, we used both GEO public datasets and our own data to analyze the expression patterns of VDAC2 and other isoforms in normal lymphoid T cells as compared to T-ALL cells. We applied two approaches to inhibit and study the function of *VDAC2* gene in the survival and proliferation of T-ALL cells, namely: by using a small molecule inhibitor of VDAC2 and secondly using a small interfering RNA (siRNA) method.

VDAC2 function is distinct among VDAC isoforms in that it dynamically interacts with pro-apoptotic BAK molecule, keeping it in check, and when dissociated from BAK, results in activation of caspase cascade and cell death [6] [15]. In this study, we explored a distinct physiological role for VDAC2 in modulating the survival and proliferation of T-cell acute lymphoblastic leukemia, thereby enhancing the leukemogenic of T-ALL cells.

Our study showed that VDAC2 is highly expressed in T-ALL cells and confirmed that protein-to-protein interactions exist between VDAC2 and BAK as well as other proteins such as BAX, BCL2-L1, CASP3 and DIABLO, associated with mitochondrial-mediated apoptosis pathway (Figure 3(B)). In contrast to previous studies involving non-malignant cells in which VDAC1 was the most expressed VDAC isoform [7] [12] [14] [17] [19] [20] [21], our results showed that VDAC2 expression levels were higher than VDAC1 in T-ALL and normal peripheral T lymphocytes, but VDAC1 remained the highest expressed isoform in haemopoietic stem cells (HPSCs) and thymocytes.

We showed that inhibiting VDAC2 in T-ALL cells either by small molecular VDAC2 inhibitor erastin or by VDAC2 siRNA resulted in a decreased proliferation rate and an increased vulnerability of T-ALL cells, to cell death. Our study demonstrated the critical role of mitochondrial VDAC2 in supporting the survival of T-ALL cells to escape apoptosis and thereby promoting proliferation. When VDAC2 protein is inhibited, this protective role is removed and results in decreased cell viability and a high apoptosis rate (Figure 6). Overall, T-ALL cells whether they were sensitive to erastin or not, suffered a dramatic < 80% decrease in viability, decreased proliferation rate and increased apoptosis rate, 72 hours post-transfection with a retrovirus vector containing VDAC2 siRNA (Figures 6(A)-(D)).

Inhibiting VDAC2 with a small inhibitor erastin reduced the viability of T-ALL cells, although only two out of nine (2/9) cell lines tested were sensitive. This result signifies a poor chemosensitivity of T-ALL cells to erastin. This is similar to the poor erastin chemosensitivity that was reported elsewhere, such as in ovarian cancer [22] and pancreatic cancer [23].

There are many advantages to using siRNA over small molecule inhibitors. Small interfering RNA (siRNA) is an RNA interference (RNAi) method for the

knocking down of endogenous genes through post-transcriptional gene silencing (PTGS). It is a specific method that interferes with the expression of specific genes with complementary nucleotide sequences by degrading mRNA after transcription, thereby preventing translation [24] [25]. It has so many advantages in studying the function of specific genes. Firstly, siRNA is specific in that it only destroys mRNA from homologous genes, and a single nucleotide change can have a significant impact on targeting and inhibition. Secondly, siRNA results in very low levels of expression of a target gene even when the concentration of siRNA given is smaller than that of antisense nucleic acids [26]. RNAi is a unique gene disruption approach that silences or inhibits the expression of the target gene and is frequently used for new gene screening, gene function identification, and gene therapy [24] [25] [26]. Therefore, it does not come as a surprise that inhibition of VDAC2 with small molecular inhibitor erastin showed poor potency in causing effects on all T-ALL cell lines than siRNA did.

However, when VDAC2 was genetically downregulated using a more sensitive and specific method of siRNA, this contrasting result from erastin-treated cells indicates that the poor chemosensitivity produced by erastin may be a result of other factors related to the pharmacodynamics and pharmacokinetics such as potency, selectivity and water solubilities of erastin as reported elsewhere [27], and not necessarily the inefficiency of VDAC2 gene deletion to decrease cell viability.

Indeed, our study further highlights the benefits of using siRNA-based therapies to limit cancer cell growth and proliferation both *in vitro* and *in vivo*, which can benefit the treatment of T-ALL, similar as reported in liver diseases siRNA-based therapeutics [28] [29]. Furthermore, siRNA-based therapies have demonstrated significant promise in sensitizing cancer cells to chemotherapy by genetically blocking genes that contribute to drug resistance during chemotherapy [28].

In addition, when T-ALL cells were transiently silenced for VDAC2 and were stained with PI method, they showed the sub-G1 stage of cell cycle (**Figure 7**), which indicates the initial stages of cell death. The inhibition of *VDAC2* led to the induction of G0/G1 cell cycle arrest, with similar flow cytometry histograms as reported elsewhere [30] [31]. Previously, studies on leukemia only used a small inhibitor erastin to inhibit VDAV2 and no other studies directly inhibited VDAC2 gene to test its role in supporting survival and proliferation.

The decrease in T-ALL cell viability following inhibition of VDAC2 as explained in literature owes to VDAC2 binding and inactivating a pro-apoptotic BCL-2 molecule, BAK and in VDAC2 absence thereof leads to BAK homo-dimerization [16] [20] [32]. Therefore, inhibiting VDAC2 releases BAX/BAK and leads to activation of apoptosis [6] [33]. Also, Chin *et al.*'s (2018) research group demonstrated that deletion of *VDAC2* accelerated tumor development by disengaging *BAX* in impairing both the killing of tumor cells by anti-cancer agents and also in the ability to suppress tumor formation [16]. Altogether, this, therefore, highlights the protection ability of *VDC2* on tumor development [16].



In conclusion, our study found that VDAC2 is highly expressed in T-ALL cells. Inhibiting VDAC2 led to a significant reduction in cell viability, increased apoptosis, decreased cell proliferation, and induced cell cycle sub-G1 arrest in T-ALL cells. Further studies are required to determine the exact mechanisms and confirm the presence of MOMP in inhibited cells.

### Acknowledgements

We would like to extend our gratitude to a number of people, very valuable in this research. Sincere gratitude to my supervisor Prof. Zou Lin and my instructor Dr. Shu Yi. I would also thank my fellow lab mates: Zhu Dan, Ma Deyu, Zeng Lamei, Hui Jun, Wang Ming, Li Bo and Liu Ziyang for their contribution to this research. This study was made possible with a grant from the Chinese Government Scholarship Council.

### Conflicts of Interest

The authors declare no conflicts of interest regarding the publication of this paper.

### References

- [1] Arber, D.A., *et al.* (2016) The 2016 Revision to the World Health Organization Classification of Myeloid Neoplasms and Acute Leukemia. *Blood*, **127**, 2391-2405. <https://doi.org/10.1182/blood-2016-03-643544>
- [2] McMahan, C.M. and Luger, S.M. (2019) Relapsed T Cell ALL: Current Approaches and New Directions. *Current Hematologic Malignancy Reports*, **14**, 83-93. <https://doi.org/10.1007/s11899-019-00501-3>
- [3] Olivas-Aguirre, M., Pottosin, I. and Dobrovinskaya, O. (2019) Mitochondria as Emerging Targets for Therapies against T Cell Acute Lymphoblastic Leukemia. *Journal of Leukocyte Biology*, **105**, 935-946. <https://doi.org/10.1002/JLB.5VMR0818-330RR>
- [4] Xu, X., *et al.* (2023) PD-1 Signalling Defines and Protects Leukaemic Stem Cells from T Cell Receptor-Induced Cell Death in T Cell Acute Lymphoblastic Leukaemia. *Nature Cell Biology*, **25**, 170-182. <https://doi.org/10.1038/s41556-022-01050-3>
- [5] Sin, C.F. and Man, P.M. (2021) Early T-Cell Precursor Acute Lymphoblastic Leukemia: Diagnosis, Updates in Molecular Pathogenesis, Management, and Novel Therapies. *Frontiers in Oncology*, **11**, Article 750789. <https://doi.org/10.3389/fonc.2021.750789>
- [6] Ren, D., *et al.* (2009) The VDAC2-BAK Rheostat Controls Thymocyte Survival. *Science Signaling*, **2**, ra48. <https://doi.org/10.1126/scisignal.2000274>
- [7] Fang, D. and Maldonado, E.N. (2018) VDAC Regulation: A Mitochondrial Target to Stop Cell Proliferation. *Advances in Cancer Research*, **138**, 41-69. <https://doi.org/10.1016/bs.acr.2018.02.002>
- [8] Neuzil, J., Pervaiz, S. and Fulda, S. (2014) Mitochondria: The Anti-Cancer Target for the Third Millennium. Springer Nature, Berlin.
- [9] Bonora, M., Giorgi, C. and Pinton, P. (2022) Molecular Mechanisms and Consequences of Mitochondrial Permeability Transition. *Nature Reviews Molecular Cell Biology*, **23**, 266-285. <https://doi.org/10.1038/s41580-021-00433-y>

- [10] Maurya, S.R. and Mahalakshmi, R. (2016) VDAC-2: Mitochondrial Outer Membrane Regulator Masquerading as a Channel? *The FEBS Journal*, **283**, 1831-1836. <https://doi.org/10.1111/febs.13637>
- [11] Naghdi, S., Varnai, P. and Hajnoczky, G. (2015) Motifs of VDAC2 Required for Mitochondrial Bak Import and tBid-Induced Apoptosis. *Proceedings of the National Academy of Sciences of the United States of America*, **112**, E5590-E5599. <https://doi.org/10.1073/pnas.1510574112>
- [12] Camara, A.K.S., Zhou, Y, Wen, P.C. and Kwok W. (2017) Mitochondrial VDAC1: A Key Gatekeeper as Potential Therapeutic Target. *Frontiers in Physiology*, **8**, Article 460. <https://doi.org/10.3389/fphys.2017.00460>
- [13] Kroemer, G., Galluzzi, L. and Brenner, C. (2007) Mitochondrial Membrane Permeabilization in Cell Death. *Physiological Reviews*, **87**, 99-163. <https://doi.org/10.1152/physrev.00013.2006>
- [14] Maldonado, E.N. (2017) VDAC-Tubulin, an Anti-Warburg Pro-Oxidant Switch. *Frontiers in Oncology*, **7**, Article 4. <https://doi.org/10.3389/fonc.2017.00004>
- [15] Tajeddine, N., *et al.* (2008) Hierarchical Involvement of Bak, VDAC1 and Bax in Cisplatin-Induced Cell Death. *Oncogene*, **27**, 4221-4232. <https://doi.org/10.1038/onc.2008.63>
- [16] Chin, H.S., *et al.* (2018) VDAC2 Enables BAX to Mediate Apoptosis and Limit Tumor Development. *Nature Communications*, **9**, Article 4976.
- [17] Arif, T., *et al.* (2014) Silencing VDAC1 Expression by siRNA Inhibits Cancer Cell Proliferation and Tumor Growth *in Vivo*. *Molecular Therapy Nucleic Acids*, **3**, e159. <https://doi.org/10.1038/mtna.2014.9>
- [18] Sioud, M. (2021) RNA Interference: Story and Mechanisms. In: Ditzel, H.J., Tutto-lomondo, M. and Kauppinen, S., Eds., *Design and Delivery of siRNA Therapeutics. Methods in Molecular Biology*, Vol. 2282, Humana, New York, 1-15. [https://doi.org/10.1007/978-1-0716-1298-9\\_1](https://doi.org/10.1007/978-1-0716-1298-9_1)
- [19] Baines, C., Kaiser, R. and Sheiko, T. (2007) Voltage-Dependent Anion Channels Are Dispensable for Mitochondrial-Dependent Cell Death. *Nature Cell Biology*, **9**, 550-555. <https://doi.org/10.1038/ncb1575>
- [20] Cheng, E.H. and Craigen, W.J. (2013) VDAC2 Inhibits BAK Activation and Mitochondrial Apoptosis. *Science*, **301**, 513-517. <https://doi.org/10.1126/science.1083995>
- [21] Heslop, K.A., Milesi, V. and Maldonado, E.N. (2021) VDAC Modulation of Cancer Metabolism: Advances and Therapeutic Challenges. *Frontiers in Physiology*, **12**, Article 742839. <https://doi.org/10.3389/fphys.2021.742839>
- [22] Cang, W., *et al.* (2022) Erastin Enhances Metastatic Potential of Ferroptosis-Resistant Ovarian Cancer Cells by M2 Polarization through STAT3/IL-8 Axis. *International Immunopharmacology*, **113**, Article ID: 109422. <https://doi.org/10.1016/j.intimp.2022.109422>
- [23] Liu, Y., *et al.* (2022) Vitamin C Sensitizes Pancreatic Cancer Cells to Erastin-Induced Ferroptosis by Activating the AMPK/Nrf2/HMOX1 Pathway. *Oxidative Medicine and Cellular Longevity*, **2022**, Article ID: 5361241. <https://doi.org/10.1155/2022/5361241>
- [24] Han, H. (2018) RNA Interference to Knock Down Gene Expression. In: DiStefano, J., Ed., *Disease Gene Identification. Methods in Molecular Biology*, Vol. 1706, Humana Press, New York, 293-302. [https://doi.org/10.1007/978-1-4939-7471-9\\_16](https://doi.org/10.1007/978-1-4939-7471-9_16)
- [25] Travella, S. and Keller, B. (2009) Down-Regulation of Gene Expression by RNA-Induced Gene Silencing. In: Jones, H. and Shewry, P., Eds., *Transgenic Wheat, Barley and Oats*, Vol. 478, Humana Press, New York, 185-199.

- [https://doi.org/10.1007/978-1-59745-379-0\\_12](https://doi.org/10.1007/978-1-59745-379-0_12)
- [26] Liu, C.Y., *et al.* (2015) Effect of siRNA Targeting HER2/Neu on the Proliferation and Viability of Prostate Cancer PC-3M Cells. *Genetics and Molecular Research*, **14**, 17145-17153. <https://doi.org/10.4238/2015.December.16.14>
- [27] Zhang, Y., *et al.* (2019) Imidazole Ketone Erastin Induces Ferroptosis and Slows Tumor Growth in a Mouse Lymphoma Model. *Cell Chemical Biology*, **26**, 623-633.e9. <https://doi.org/10.1016/j.chembiol.2019.01.008>
- [28] Friedrich, M. and Aigner, A. (2022) Therapeutic siRNA: State-of-the-Art and Future Perspectives. *BioDrugs*, **36**, 549-571. <https://doi.org/10.1007/s40259-022-00549-3>
- [29] Holm, A., Lovendorf, M.B. and Kauppinen, S. (2021) Development of siRNA Therapeutics for the Treatment of Liver Diseases. In: Ditzel, H.J., Tuttolomondo, M. and Kauppinen, S., Eds., *Design and Delivery of SiRNA Therapeutics*. Methods in Molecular Biology, Vol. 2282, Humana, New York, 57-75. [https://doi.org/10.1007/978-1-0716-1298-9\\_5](https://doi.org/10.1007/978-1-0716-1298-9_5)
- [30] Bao, J., *et al.* (2020) Scutellarin Exerts Anticancer Effects on Human Leukemia Cells via Induction of Sub-G1 Cell Cycle Arrest, Apoptosis and Also Inhibits Migration and Invasion by Targeting Raf/MEK/ERK Signalling Pathway. *Journal of Balkan Union of Oncology*, **25**, 1050-1055.
- [31] Zhuang, W., *et al.* (2011) The Mechanism of the G0/G1 Cell Cycle Phase Arrest Induced by Activation of PXR in Human Cells. *Biomedicine & Pharmacotherapy*, **65**, 467-473. <https://doi.org/10.1016/j.biopha.2011.04.014>
- [32] Ma, S.B., *et al.* (2014) Bax Targets Mitochondria by Distinct Mechanisms before or during Apoptotic Cell Death: A Requirement for VDAC2 or Bak for Efficient Bax Apoptotic Function. *Cell Death & Differentiation*, **21**, 1925-1935. <https://doi.org/10.1038/cdd.2014.119>
- [33] Walensky, L.D. (2019) Targeting BAX to Drug Death Directly. *Nature Chemical Biology*, **15**, 657-665. <https://doi.org/10.1038/s41589-019-0306-6>